

# Surface and Bulk Properties of Chromium Oxide: Implications for Reduction by Methane

Kristin M. Skjelbred\*, Per-Olof Åstrand\*, Jon Andreas Støvneng<sup>†</sup> and Stefan Andersson\*\*

\*Department of Chemistry, Norwegian University of Science and Technology (NTNU), 7491 Trondheim, Norway

<sup>†</sup>Department of Physics, Norwegian University of Science and Technology (NTNU), 7491 Trondheim, Norway

\*\*SINTEF Materials and Chemistry, P. O. Box 4760, 7465 Trondheim, Norway

**Abstract.** A computational method for  $\text{Cr}_2\text{O}_3$  and  $\text{Cr}_3\text{C}_2$  has been established based on a systematic investigation of functionals, basis sets and corrections for dispersion, self-interaction and relativistic effects. The suggested method comprises of the PBE functional with Grimme's dispersion correction, the TZ2P basis set with a frozen core of up to  $2p$  for chromium and  $1s$  for oxygen and carbon, and with the zeroth-order regular approximation for relativistic effects, and is in good agreement with experimental results for both bulk crystals and surface structures. Self-interactions have been corrected for by the DFT +  $U$  approach, but it still gives band gaps significantly different from the experimental band gap. We have also calculated the adsorption energy of methane on a chromium terminated (0001)  $\text{Cr}_2\text{O}_3$  surface, and the significance of dispersion and self-interaction corrections for the adsorption of methane on  $\text{Cr}_2\text{O}_3$  was found to be substantial.

**Keywords:** density functional theory, chromium oxide, adsorption

**PACS:** 61.50.Ah, 68.43.Bc, 71.15.Mb, 82.65.+r

## INTRODUCTION

The aim of our work is to determine how chromite ores successfully can be reduced by methane by using quantum chemical methods and simulations. Several studies show that  $\text{Cr}_2\text{O}_3$  readily is reduced to  $\text{Cr}_3\text{C}_2$  by methane gas [1, 2]. This process can take place at lower temperatures than when solid carbon is used. There is, however, no obvious explanation as to why the situation is different for chromite ores. To better understand how different properties affect the way  $\text{Cr}_2\text{O}_3$  and chromite ores react with methane, we need a rigorous method that describes the electronic structure, geometry and reaction rate constants accurately. Density functional theory (DFT) is an efficient method for both electronic structure calculations and geometry optimizations of molecules, and it is also transferable to periodic systems such as surfaces. Periodic DFT enables investigation of different terminations of the surface, and can be used together with molecular DFT to calculate the adsorption energy of atoms and molecules on the surface. Even though both many wavefunction methods and DFT struggle to treat systems with multi-reference character, DFT is better suited for systems of this magnitude.

It is well known that transition metal chemistry, like rare earth metals, introduces new challenges in computational chemistry compared to systems made up of purely main group elements [3]. As the initial aim is to assess a suitable DFT method for describing the interaction between  $\text{Cr}_2\text{O}_3$  and  $\text{CH}_4$ , the most relevant errors will be the ones that are not cancelled when adsorption and reaction energies are calculated. The energy for reaction  $j$  is determined by

$$E_j = E^{\text{products}} - E^{\text{reactants}} \quad (1)$$

where  $E^{\text{products}}$  and  $E^{\text{reactants}}$  are the sums of the energy of formation for each species.

One issue is the electron correlation arising from the near-degeneracy of the  $4s$  and partially filled  $3d$  orbitals, which has an effect on the ground-state structure and energy of the system. For solids containing TMs the bandgaps are strongly underestimated due to self-interaction errors. There are several ways to correct for it in DFT [4, 5, 6], and the DFT +  $U$  approach [7, 8] has been tested in this work. The DFT +  $U$  energy includes a correction for the on-site Coulomb interactions for the  $3d$ -orbitals through the system specific parameter,  $U$ ,

$$E^{\text{DFT+U}} = E^{\text{DFT}} + \frac{U}{2} \sum_{m,\sigma} [n_{m,\sigma}^{\sigma} - \sum_{m'} n_{m,m'}^{\sigma} n_{m',m}^{\sigma}] \quad (2)$$

where  $U$  is a sum over the spherically averaged matrix elements of the on-site Coulomb interactions  $\bar{U}$  and  $\bar{J}$ .  $n$  is the on-site  $3d$ -orbital occupation matrix obtained by projection of the wavefunction onto  $3d$  atomic like states, while  $m$  and  $m' = -2, -1, 0, 1, 2$  denote the  $d$ -orbitals and  $\sigma$  the spin.

When the velocity of an electron approaches the speed of light, relativistic effects should be taken into consideration [9]. Although the effect is important for heavy atoms, the zeroth-order regular approximation (ZORA) to the Dirac equation can be applied without increasing the computational complexity significantly, and is therefore commonly used for most systems [10, 11]. Another possibility is to use pseudopotentials that are parametrized with a frozen core, a semi frozen core for the valence electrons, as well as a relativistic correction [12].

In the general gradient approximation (GGA), there are difficulties describing long-range interactions, such as dispersion. As the purpose of this work is to find a DFT model that gives a reasonable description of the interaction between molecules and surfaces, dispersion corrected exchange-correlation functionals are also tested [13, 14].

## COMPUTATIONAL DETAILS

Using the ADF molecular modelling suite [15] and Quantum Espresso [16], we have compared Slater-type orbital basis sets and plane waves. The initial magnetic ordering of the chromium layers is set as antiferromagnetic, unless something else is specified.

In ADF BAND we have investigated the basis set dependence for the following basis sets, TZP, TZ2P and QZ4P [17]. To investigate the effect of dispersion interaction different versions of Grimme’s [13, 14] dispersion corrections to the Perdew-Becke-Ernzerhof (PBE) functional [18] have been added. A short hand notation for the different models is used. For instance PBE with Grimme’s D3 correction, the TZ2P basis set with a frozen core of up to  $2p$  for chromium and  $1s$  for oxygen would be denoted PBE-D3/TZ2P.2p.1s.

For the calculations done with Quantum Espresso the Vanderbilt ultrasoft pseudopotentials [12] were used together with the PW91 functional [19]. The kinetic energy cutoff for the wavefunctions and charge density was set to 25.0 and 240.0 (Ry) respectively and a  $k$ -point mesh of  $4 \times 4 \times 4$  over the irreducible Brillouin zone, according to the Monkhorst-Pack scheme was used [20].

### Bulk $\text{Cr}_2\text{O}_3$

$\text{Cr}_2\text{O}_3$  has  $R\bar{3}c$  symmetry, and can be described by a rhombohedral unit cell or using hexagonal cell parameters,  $a$  and  $c$ . The oxygen atoms are positioned in hexagonal close packed layers, while the chromium atoms occupy  $2/3$  of the octahedral holes between each layer [21]. The internal structure of the unit cell is described by the Wyckoff parameters  $x$  for oxygen and  $z$  for chromium.

The geometry of the rhombohedral unit cell was optimized with the PBE functional for the TZP.2p.1s, TZ2P.2p.1s and QZ4P.2p.1s basis sets. The band gap is significantly smaller compared to the experimental value of 3.4 eV [22], as expected from DFT without any correction for self-interactions for transition metal oxides. For all the three basis sets the band gap was estimated to be 1.6 eV. Looking at the geometry of the unit cell, however, TZ2P.2p.1s is in good agreement with experimental values ( $a=4.961$  Å,  $c=13.599$  Å,  $x=0.306$  Å and  $z=0.348$  Å) [21]. While  $a$  was underestimated by 0.009 Å,  $c$  was overestimated by 0.211 Å. Including an all-electron TZ2P basis set resulted in a marginal improvement of the band gap,  $a$ ,  $z$  and  $x$ , while  $c$  was overestimated even more compared to the parameters obtained from the frozen core calculation. Over all there was no significant improvement doing an all electron calculation and  $1s$  for oxygen and all orbitals up to  $2p$  for chromium will therefore be kept frozen in the following calculations.

The contribution from relativistic effects, by ZORA, is relatively small for this system. It does, however, improve the model and the cost of including it in the model is practically zero. Two additional functionals were tested. The revised PBE (RPBE) [23] functional is designed to describe atomization energies of molecules during chemisorption on transition-metal surfaces more accurately than PBE. The HTBS [24] functional retains the atomization energies from RPBE, while giving a better description of the lattice constants for solids. We found that RPBE gave an  $a/c$  ratio closer to experiment, but both  $a$  and  $c$  were overestimated, while HTBS underestimated  $a$  by 0.066 Å and overestimated  $c$  by 0.135 Å. Overall, the three functionals give similar results.

Optimizing the geometry with PBE-D/TZ2P.2p.1s and PBE-D3/TZ2P.2p.1s, without relativistic effects did, as expected, give similar results as PBE for the bulk crystal. PBE-D underestimated  $a$  by 0.035 Å, and  $c$  was overestimated

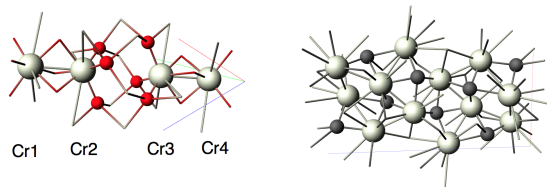


**FIGURE 1.** Rhombohedral unit cell of Cr<sub>2</sub>O<sub>3</sub> (left), and orthorhombic unit cell of Cr<sub>3</sub>C<sub>2</sub> (right). Chromium atoms are white, oxygen red, and carbon grey.

by 0.054 Å compared to experimental values [21]. PBE-D3 gave the same trend with the changes of 0.038 Å and 0.166 Å, respectively. The internal cell coordinates differed with less than 0.001 Å compared to no dispersion correction.

Considering the energy for different magnetic configurations relative to the antiferromagnetic state, where Cr1 and Cr3 have  $\alpha$  spin and Cr2 and Cr4  $\beta$  spin (see Figure 1), it was confirmed that the antiferromagnetic state is the ground state. Two other antiferromagnetic orderings were also considered, but were higher in energy. The ferromagnetic ordering gave the highest energy, while setting the spin of only one of the chromium atoms opposite to the three remaining ones gave an intermediate energy increase.

Quantum Espresso retains an  $a/c$  ratio closer to experiment [21]. While  $a$ ,  $c$  and  $z$  are underestimated by 0.092 Å, 0.226 Å and 0.003 Å respectively,  $x$  is overestimated by 0.009 Å compared to experiment [21]. Addition of the  $U$  term to the energy gave an improvement of the band gap from 1.62 eV for  $U = 0$  eV to 2.54 eV for  $U = 4.0$  eV and 2.75 eV for  $U = 7.7$  eV.

## Bulk Cr<sub>3</sub>C<sub>2</sub>

The Cr<sub>3</sub>C<sub>2</sub> unit cell has an orthorhombic structure, so all three lattice parameters,  $a$ ,  $b$  and  $c$  need to be specified. The chromium and carbon atoms both possess  $4c$  symmetry, with three inequivalent Cr atoms in the  $(x, 1/4, z)$  positions and two inequivalent C atoms in the  $(x, 3/4, z)$  positions [25].

PBE-D3/TZ2P.2p.1s and ZORA gives a description of the unit cell in good agreement with experiment [26]. The lattice parameter  $a$  is overestimated by 0.0026 Å, while  $b$  and  $c$  are underestimated by 0.078 and 0.014 Å, respectively, compared to experiment.

## Cr<sub>2</sub>O<sub>3</sub> Surfaces

The optimized geometry of the bulk crystal was used to create a slab in the (0001) direction, with three Cr<sub>2</sub>O<sub>3</sub> layers. During the optimization of the slab the geometry of the two lowest oxygen layers and the lowest chromium layers were kept fixed, while the top layers were allowed to relax. In the unit cell each chromium layer consists of two inequivalent chromium atoms, while the oxygen layers each consist of three oxygen atoms. All the calculations in this section have been done using ADF BAND with PBE-D3/TZ2P.2p.1s and ZORA.

Two Cr-terminated surfaces were considered, one with a Cr<sub>2</sub>-layer, and another where half of the Cr-atoms have been removed, the latter being the more commonly studied surface termination of (0001) Cr<sub>2</sub>O<sub>3</sub> surfaces [27, 28]. Several oxygen terminated surfaces have been studied [29, 30], and we have included ...-Cr<sub>2</sub>O<sub>3</sub>CrO, ...-Cr<sub>2</sub>O<sub>3</sub>CrO<sub>3</sub> and ...-CrO<sub>3</sub>Cr<sub>3</sub>O<sub>3</sub> in our study. For a reference on the notation, see ref. [29].

The adsorption energy,  $E^{\text{ad}}$ , of methane on the Cr<sub>2</sub>O<sub>3</sub> surface has been computed by optimizing the geometry for a slab, obtaining  $E^{\text{slab}}$ , a molecule, obtaining  $E^{\text{mol}}$ , and the molecule bound to the surface, obtaining  $E^{\text{bound}}$ . The adsorption energy is given by

$$E^{\text{ad}} = (E^{\text{slab}} + E^{\text{mol}}) - E^{\text{bound}} \quad (3)$$

i.e.  $E^{\text{ad}}$  is positive when adsorption is favored. The calculated adsorption energies for the ...-O<sub>3</sub>Cr<sub>2</sub> and the ...-O<sub>3</sub>Cr terminated surfaces are 0.175 eV and 0.228 eV, respectively with PBE-D3/TZ2P.2p.1s. Omitting the dispersion correction results in 0.94 eV, and an addition of the  $U$  term gives 0.369 eV, showing the significance of dispersion and self-interaction corrections. The distance between the carbon atom in methane and the top chromium atom is over 3 Å

for both surface structures, which is longer than what would be considered a covalent C-Cr bond. The smallest unit cell possible was used for the calculations, meaning one CH<sub>4</sub> molecule per Cr<sub>2</sub> or Cr atom on the top layer, and the effect of coverage should be investigated in more detail.

## CONCLUSIONS

The PBE-D3/TZ2P.2p.1s model results in lattice parameters in good agreement with experiment for both Cr<sub>2</sub>O<sub>3</sub> and Cr<sub>3</sub>C<sub>2</sub>, and antiferromagnetic ordering of the chromium atoms is confirmed as the ground state. The model was also tested for different terminations of the (0001) Cr<sub>2</sub>O<sub>3</sub> surface and lead to the expected relaxation of the top layers of the in the surface structure of the slabs, in accordance with experiments and previous computational models. Through calculations of the adsorption energy of CH<sub>4</sub> on a chromium terminated surface, it is found that adsorption is favored. Dispersion interactions contribute significantly and self-interaction errors cannot be ignored.

## ACKNOWLEDGMENTS

This work has been funded by the Norwegian Research Council (NFR) through the GASSMAKS project (grant no 233825), and enabled by computer time from the Norwegian High Performance Computing Consortium (NOTUR), account nn2920k.

## REFERENCES

1. N. Anacleto, and O. Ostrovski, *Metall. Mater. Trans. B* **35B**, 609–615 (2004).
2. O. Ostrovski, and G. Zhang, *Am. Inst. Chem. Eng.* **52**, 300–310 (2006).
3. C. J. Cramer, and D. G. Truhlar, *Phys. Chem. Chem. Phys.* **11**, 10757–10816 (2009).
4. J. P. Perdew, and A. Zunger, *Phys. Rev. B* **23**, 5048 (1981).
5. F. Aryasetiawan, and O. Gunnarson, *Phys. Rev. Lett.* **101**, 066403 (1995).
6. F. Tran, and P. Blaha, *Phys. Rev. Lett.* **102**, 226401 (2009).
7. V. I. Anismov, J. Zaanen, and O. K. Andersen, *Phys. Rev. B* **44**, 943 (1991).
8. V. I. Anismov, F. Aryasetiawan, and A. I. Lichtenstein, *J. Phys. Cond. Matt.* **9**, 767 (1997).
9. P. Pyykkö, *Annu. Rev. Phys. Chem.* **63**, 45 (2012).
10. E. van Lenthe, E. J. Baerends, and J. G. Snijders, *J. Chem. Phys.* **99**, 4597–4610 (1993).
11. E. van Lenthe, A. E. Ehlers, and E. J. Baerends, *J. Chem. Phys.* **110**, 8943 (1999).
12. D. Vanderbilt, *Phys. Rev. B* **41**, 7892 (1990).
13. S. Grimme, *J. Comp. Chem.* **27**, 1787–1799 (2006).
14. S. Grimme, J. Anthony, S. Ehrlich, and H. Krieg, *J. Chem. Phys.* **132**, 154104 (2010).
15. G. te Velde, F. M. Bickelhaupt, E. J. Baerends, C. F. Guerra, S. J. A. van Gisbergen, J. G. Snijders, and T. Ziegler, *J. Comp. Chem.* **22**, 931 (2001).
16. P. Giannozzi, S. Baroni, N. Bonini, M. Calandra, R. Car, D. C. C. Cavazzoni and, G. L. Chiarotti, M. Cococcioni, I. Dabo, A. D. Corso, S. de Gironcoli, S. Fabris, G. Fratesi, R. Gebauer, U. Gerstmann, C. Gougoussis, A. Kokalj, M. Lazzeri, L. Martin-Samos, N. Marzari, F. Mauri, R. Mazzarello, S. Paolini, A. Pasquarello, L. Paulatto, C. Sbraccia, S. Scandolo, G. Sclauzero, A. P. Seitsonen, A. Smogunov, P. Umari, and R. M. Wentzcovitch, *J. Phys. Cond. Matt.* **21**, 395502 (2009).
17. E. van Lenthe, and E. J. Baerends, *J. Comput. Chem.* **24**, 1142–1156 (2003).
18. J. P. Perdew, K. Burke, and M. Ernzerhof, *Phys. Rev. Lett.* **77**, 3865–3868 (1996).
19. J. P. Perdew, J. A. Chevary, S. H. Vosko, K. A. Jackson, M. R. Pederson, D. J. Singh, and C. Fiolhais, *Phys. Rev. B* **46**, 6671–6687 (1992).
20. H. J. Monkhorst, and J. D. Pack, *Phys. Rev. B* **13**, 5188 (1976).
21. R. E. Newnham, and Y. M. D. Haan, *Z. Naturforsch* **117**, 235–237 (1962).
22. J. A. Crawford, and R. W. Vest, *J. Appl. Phys.* **35**, 2413 (1964).
23. B. Hammer, L. B. Hansen, and J. K. Nørskov, *Phys. Rev. B* **59**, 7413 (1999).
24. P. Haas, F. Tran, P. Blaha, and K. Schwarz, *Phys. Rev. B* **83**, 205117 (2011).
25. S. Rundqvist, and G. Runnsjö, *Acta Chem. Scand.* **23**, 1191 (1969).
26. J. Glaser, R. Schmitt, and H.-J. Meyer, *Z. Naturforsch* **58b**, 929 (2003).
27. C. Rehbein, N. M. Harrison, and A. Wander, *Phys. Rev. B* **54**, 14066 (1996).
28. R. Rohr, M. Bäumer, H. Freund, J. A. Meijas, V. Staemmler, S. Müller, L. Hammer, and K. Heinz, *Surf. Sci.* **389**, 391 (1997).
29. A. Rohrbach, J. Hafner, and G. Kresse, *Phys. Rev. B* **70**, 125426 (2004).
30. K. N. Nigussa, K. L. Nielsen, Ø. Borck, and J. A. Støvneng, *Corr. Sci.* **53**, 3612–3622 (2011).